Journal of Chemistry and Technologies, 2024, *32*(1), 108-118

Journal of Chemistry and Technologies

pISSN 2663-2934 (Print), ISSN 2663-2942 (Online).

journal homepage: http://chemistry.dnu.dp.ua
editorial e-mail: chem.dnu@gmail.com

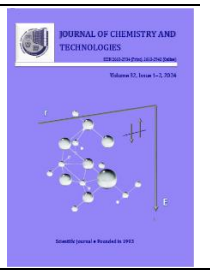

UDC 661.097.3

STUDY OF THE INFLUENCE OF SYNTHESIS PARAMETERS ON THE STRUCTURAL AND MAGNETIC PROPERTIES OF COBALT FERRITE

Liliya A. Frolova*, Irina V. Sknar
Ukrainian State University of Chemical Technology, Dnipro, Ukraine
Received 11 February 2024; accepted 16 March 2023; available online 25 April 2024

Abstract

The paper proposes the use of contact low-temperature non-equilibrium plasma for the synthesis of cobalt ferrite. The influence of the pH of the reaction medium, temperature, and duration of treatment on magnetic properties, the intensity of X-ray diffraction peaks, the average size of crystallites, and the value of dislocation density were determined using the central composite rotary design of the experiment. The results of X-ray phase analysis, vibrational magnetometry, and electron microscopy were used to create the models. The results showed that the pH of the reaction medium is the parameter that has the greatest influence on the growth of cobalt ferrite powder crystallites and the magnetic properties of the samples. It was established that the largest size of crystallites (505–560 Å) was obtained at high temperatures and pH values. The smallest crystallite size (119–165 Å) was obtained at a temperature of 20 °C, a minimum processing time of 5 minutes, and a pH of 10. Based on the analysis of hysteresis curves, it is shown that high values of magnetization saturation (120–138 Emu/g) can be achieved at an elevated temperature of 40 °C and processing time. This is due to the formation of cobalt ferrite with high crystallinity and large crystallite sizes. Smaller values of saturation magnetization (8–14 Emu/g) are due to the formation of non-magnetic impurity phases of iron oxides and oxyhydroxides.

Keywords: cobalt ferrite; plasma chemical synthesis; X-ray phase analysis; experimental planning; saturation magnetization; crystallite size.

ДОСЛІДЖЕННЯ ВПЛИВУ ПАРАМЕТРІВ СИНТЕЗУ НА СТРУКТУРНІ ТА МАГНІТНІ ВЛАСТИВОСТІ ФЕРИТУ КОБАЛЬТУ

Лілія А. Фролова, Ірина В. Скнар
ДВНЗ «Український державний хіміко-технологічний університет»

Анотація

Досліджений вплив параметрів синтезу на структурні та магнітні властивості фериту кобальту. В роботі досліджено синтез фериту кобальту плазмохімічним методом. Визначений вплив pH реакційного середовища, температури і тривалості обробки на магнітні властивості, інтенсивність піків на рентгенограмі, середній розмір кристалітів, значення густини дислокацій за допомогою центрального композиційного ротатабельного планування експерименту, що базується на результатах, отриманих методом рентгенофазового аналізу, вібраційної магнітометрії, електронної мікроскопії. Статистичний аналіз дав можливість кількісно оцінити вплив параметрів синтезу на обрані функції відгуку. Результати показали, що pH реакційного середовища є параметром, який оказує найбільший вплив як на ріст кристалітів порошків фериту кобальту, так і на магнітні властивості зразків, отриманих плазмохімічним методом.

Ключові слова: ферит кобальту; плазмохімічний синтез; рентгенофазовий аналіз; планування експерименту; намагніченість насичення; розмір кристалітів.

**Corresponding author: e-mail: domosedi@i.ua*

doi: 10.15421/jchemtech.v32i1.298377

Journal of Chemistry and Technologies, 2024, *32*(1), 108-118

Introduction

The huge demand for nano-sized ferrites causes significant attention of scientists to the development of technologies for their synthesis and the study of physico-chemical properties [1–3]. Among the spinel ferrites, $CoFe_2O_4$ occupies a special place due to its chemical stability, high mechanical parameters, specific electrical, magnetic, and catalytic properties, which makes it possible to use the material in many fields of application [4–8]. Cobalt ferrite is widely used in gas sensors [9–11], in medicine [15–17], and in catalytic processes of organic synthesis [18]. First of all, this is related to the nanoscale characteristics of the obtained product, which depends on the production technology and the parameters of its implementation [19]. The analysis of literary sources showed the effective use of sol-gel technology [20], coprecipitation, ceramic technology, solvothermal synthesis [21]. Determination of the parameters that have a certain influence on the synthesis process, as well as the optimal conditions of such parameters, are of crucial importance for obtaining $CoFe_2O_4$ with a controlled phase composition and structural parameters. In work [22] cobalt ferrites obtained by three processes (co-precipitation from aqueous solutions, co-precipitation in the medium of microemulsions and thermal decomposition of organometallic complexes) were considered, and it was found that the degree of spinel inversion and, accordingly, the magnetic properties are determined by the chosen synthesis method. Studies of the effect of annealing temperature on the production of cobalt ferrite showed that the maximum coercive force (1654.25 Oe) was observed for the sample annealed in the shortest time (2 hours) and at the lowest temperature (550 °C) [23].

The authors [24] found that variations in the density of defects and the shape of nanocrystals determine the distribution of switching fields and the effective magnetic anisotropy, which reaches $\approx 1 \times 107$ Erg·cm^{-3} for 9 nm cobalt ferrite nanoparticles coated with oleic acid. It is shown that the values of saturation magnetization for nanoparticles obtained by various methods are in the range from 49 to 95 Emu/g due to differences in stoichiometry, distribution of cations by sublattices. The opposite dependence of the increase in coercive force and saturation magnetization with increasing firing temperature (600, 700, and 800 °C) is described in [25].

Studies of cobalt ferrite nanoparticles synthesized by the hydrothermal method have shown that with an increase in the annealing temperature, both the saturation magnetization and the residual magnetization increase, as well as the coercive force decreases, which is associated with the transition from single-domain to multi-channel. the structure at the intersection with a critical size of ~40 nm [26]. A similar dependence was also established in [27]. The authors considered the dependence of the structural and magnetic properties of co-precipitated cobalt ferrite on the calcination temperature. As the firing temperature increases, the crystallite size increases. In addition, the results of the X-ray phase analysis indicate that the redistribution of cations occurs with an increase in the firing temperature. As a result, the saturation magnetization increases with increasing calcination temperature and reaches 62.30 Emu/g.

The authors [28; 29] established that the oxidation process also has a certain influence on the magnetic, phase and structural properties of the final product.

For example, cobalt ferrite nanoparticles with a size of 7–20 nm were synthesized by the microwave hydrothermal method with rapid heating at 100, 150, and 200 ℃ [30]. The magnitude of the saturation magnetization increases, but the final magnetization and coercive force decrease with increasing melting temperature.

That is, despite the large number of works devoted to the improvement of cobalt ferrite synthesis technologies, information on the consideration of this scientific issue is currently insufficient. The required dependences can be obtained by constructing experiments that allow one to evaluate the influence of several factors on the response function simultaneously.

This work is devoted to the study of the synthesis of cobalt ferrite by the plasma chemical method and the study of the influence of the synthesis parameters on the phase composition, crystallite size, dislocation density and magnetic properties.

Experimental

Samples were obtained by pouring with continuous stirring the appropriate mixture of 0.5 M solutions of cobalt(II) sulfate, ferrum(II) sulfate with the required molar ratio of cobalt to ferrum cations (1 : 2). The necessary pH was obtained by adding a 1M NaOH solution, followed by treatment with a plasma discharge. The description of the installation is given in [31].

Journal of Chemistry and Technologies, 2024, *32*(1), 108-118

Measurements of the solution temperature were carried out in the reactor using a thermocouple; regulation was carried out by changing the water flow in the jacket.

The concentration of cobalt cations was determined complexometrically, ferrum cations - by permanganate and bichromate methods. To control the course of the reaction, the reactor was equipped with an electrode system, which includes an ESL 43-07 glass electrode for measuring pH, a platinum electrode for measuring the oxidation potential, and an EVL-1M3 reference electrode. All sieges were washed to a negative reaction for sulfate ion. After exposure, the siege was separated by magnetic separation. The washed and filtered sediments were dried at a temperature of 130 ℃. The relative magnetic properties were determined by a vibrating magnetometer. The saturation magnetization was determined from the constructed hysteresis loop. X-ray phase analysis was performed on a DRON-3 X-ray diffractometer in monochromatized Co-Kα radiation (λ = 1.7902 Å). Identification of compounds was carried out by comparing the interplanar positions (d, Å) and relative intensities (I/I_0) of the experimental curve according to the data of the PCPDFWIN electronic card. Shooting was carried out at angles of 10-90 degrees. Phase analysis was carried out in steps of 0.1 degrees, duration 5 s. Structural analysis was carried out in steps of 0.01 degrees, duration 5 seconds. The size of the crystallites was determined by the formula:

$$L_{HKL} = \frac{0.94\lambda}{\beta Cos\,\theta_{HKL}}, \quad (1)$$

L – size of crystallites, Å

2θ – scanning angle corresponding to the position of the maximum in degrees.

The density of dislocations was determined using the quadratic dependence of the density of dislocations on the true line broadening:

$$D_{311}=A\beta^2 \quad (2)$$

D_{311} – density of reflection dislocations (311),

β – true extension of the line (311),

A is a coefficient that depends on the elastic properties of the material and the dislocation characteristics.

On the basis of previous experiments, we selected the initial pH of the solution, the plasma discharge treatment time, and the temperature of the process as the main technological parameters affecting the magnetic properties. The following values of influencing factors were proposed as boundary conditions (Table 1).

Table 1

Influential factors and their values in real form

Factor	Name	Unit of measurement	Value	
			maximum	minimum
X_1	Temperature	^{0}C	40.0	20.0
X_2	time	min	20.0	5.0
X_3	pH		12.0	8.0

Table 2

Central composite rotatable design (CCRD) in coded and real form

№	Encoded values parameters			Real values parameters		
	t	τ	pH	t, ℃	τ, min	pH
1	1	1	1	40.0	20.0	12.0
2	–1	1	1	20.0	20.0	12.0
3	1	–1	1	40.0	5,0	12.0
4	–1	–1	1	20.0	5.0	12.0
5	1	1	–1	40.0	20.0	8.0
6	–1	1	–1	20.0	20.0	8.0
7	1	–1	–1	40.0	5.0	8.0
8	–1	–1	–1	20.0	5.0	8.0
9	1.68	0	0	46.8	12.5	10.0
10	–1.68	0	0	13.2	12.5	10.0
11	0	1.68	0	30.0	25.1	10.0
12	0	–1.68	0	30.0	0.1	10.0
13	0	0	1.68	30.0	12.5	13.4
14	0	0	–1.68	30.0	12.5	6.6
15	0	0	0	30.0	12.5	10.0
16	0	0	0	30.0	12.5	10.0
17	0	0	0	30.0	12.5	10.0
18	0	0	0	30.0	12.5	10.0

Journal of Chemistry and Technologies, 2024, *32*(1), 108-118

To study the influence of synthesis parameters on the magnetic characteristics of cobalt ferrite obtained under the action of a plasma discharge, a complete three-factor experiment plan of type 2^3, supplemented with star points, was created (table 2).

In Table 2, (–1), (+1) represent the coded values of the coefficients for the minimum and maximum levels, respectively. A central composite rotatable 2^3 factorial design was used to process the experimental data consisting of 8 trials (1 and +1), 4 central points, and 6 axial points (1.68 and +1.68), resulting in an orthogonal distribution for a total of 18 experiments.

For a complete 3-factor experiment, the mathematical equation describing this system is:

$$y_i = \beta_0 + \beta_1 x_1 + \beta_2 x_2 + \beta_3 x_3 + \beta_{12} x_1 x_2 + \beta_{13} x_1 x_3 + \beta_{23} x_2 x_3 + \beta_{123} x_1 x_2 x_3 + \beta_{11} x_1^2 + \beta_{22} x_2^2 + \beta_{33}^2 \quad (3)$$

where yi is the dependent variable (response function),

β_0, β_1, β_2, β_3 are coefficients corresponding to independent variables,

β_{11}, β_{22}, β_{33} are coefficients corresponding to the squares of the independent variables,

β_{123} is coefficient of triple interaction of independent variables,

β_{12}, β_{23}, β_{13} are coefficients for pairwise interactions of independent variables.

Calculation of the model and subsequent optimization were performed using the STATSGRAPHICS 10.0 program. The obtained models were tested for the significance of factors, adequacy of the model according to Fisher's test, analysis of variance, analysis of Paretto charts.

Table 2 shows the matrix for conducting a full factorial experiment, which is used to study the effect of the plasma discharge on the values of the response functions (values of saturation magnetization (M_s), crystallite size for the plane (311) (L), density of reflection dislocations (311) (D), the intensity of the peaks on the X-ray patterns ($I_{X\text{-ray pic}}$) obtained for the coded conditions adopted in each experiment in accordance with the serial number of the samples.

Results and discussion

Fig. 1 shows X-ray patterns obtained for plasma chemically synthesized samples. X-ray patterns of samples 1, 2, 4 show only crystalline ferrite $CoFe_2O_4$ with a spinel-type cubic structure with space group Fd-3m, according to ICDD card 22-1086 (peaks correspond to d=4.88, 2.94, 2.51, 2.08, 1.7, 1.61, 1.48, 1.322 A). Additional peaks corresponding to hematite are observed at pH=8. For example, in sample 3, a small amount of α-Fe_2O_3 is present, which can be seen from the low intensity of the corresponding peaks.

Samples obtained at pH=8 show broader peaks than samples obtained at pH=12, indicating a smaller crystallite size. Samples obtained at pH = 12 have more intense peaks, which is characteristic of a highly crystallized phase (Fig. 1(a, b, c, d)).

Table 3

Results of the study of sample properties

№	Feedback function			
	M_S Emu/g	$L_{(311)}$, Å	$I_{X\text{-ray pic (311)}}$	$D*10^{-10}$, cm^{-2}
1	138.1	462	410	34.3
2	118.1	506	480	28.6
3	66.1	429	380	39.9
4	53.2	437	320	38.3
5	65.9	246	198	120.9
6	8.1	165	96	267.0
7	25.9	195	98	191.0
8	13.4	209	78	258.0
9	81.9	335	282	78.0
10	39.4	328	234	154.0
11	97.2	356	322	102.0
12	24.9	309	192	136.0
13	116.2	544	493	14.0
14	6.02	119	22.4	264.0
15	61.02	330	258	120.0
16	58.3	331	250	122.0
17	59.4	332	254	124.0
18	59.3	331	254	124.0

Journal of Chemistry and Technologies, 2024, *32*(1), 108-118

Comparing the samples synthesized at t=20 °C (Fig. 1b, 2d, 2f, 2h), only the samples synthesized at the maximum levels of pH and time showed quite intense peaks.

The isolines presented in Fig. 2 (a, b, c) confirm that the degree of crystallinity increases with increasing temperature, pH, and treatment time. Moreover, it is the pH value of the medium that has the greatest influence.

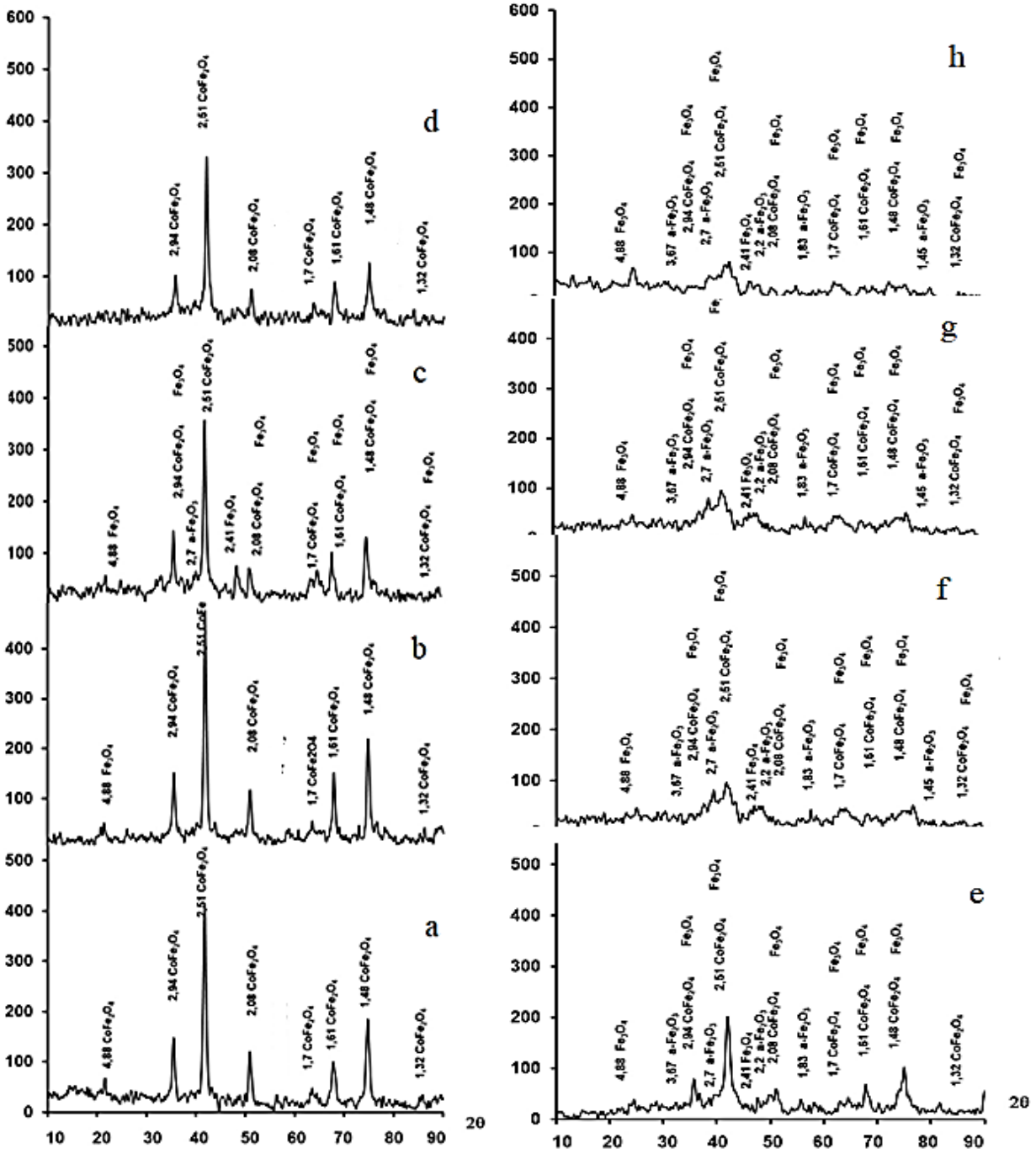

Fig.1. X-ray pattern for sample (numbering according to Table 1)

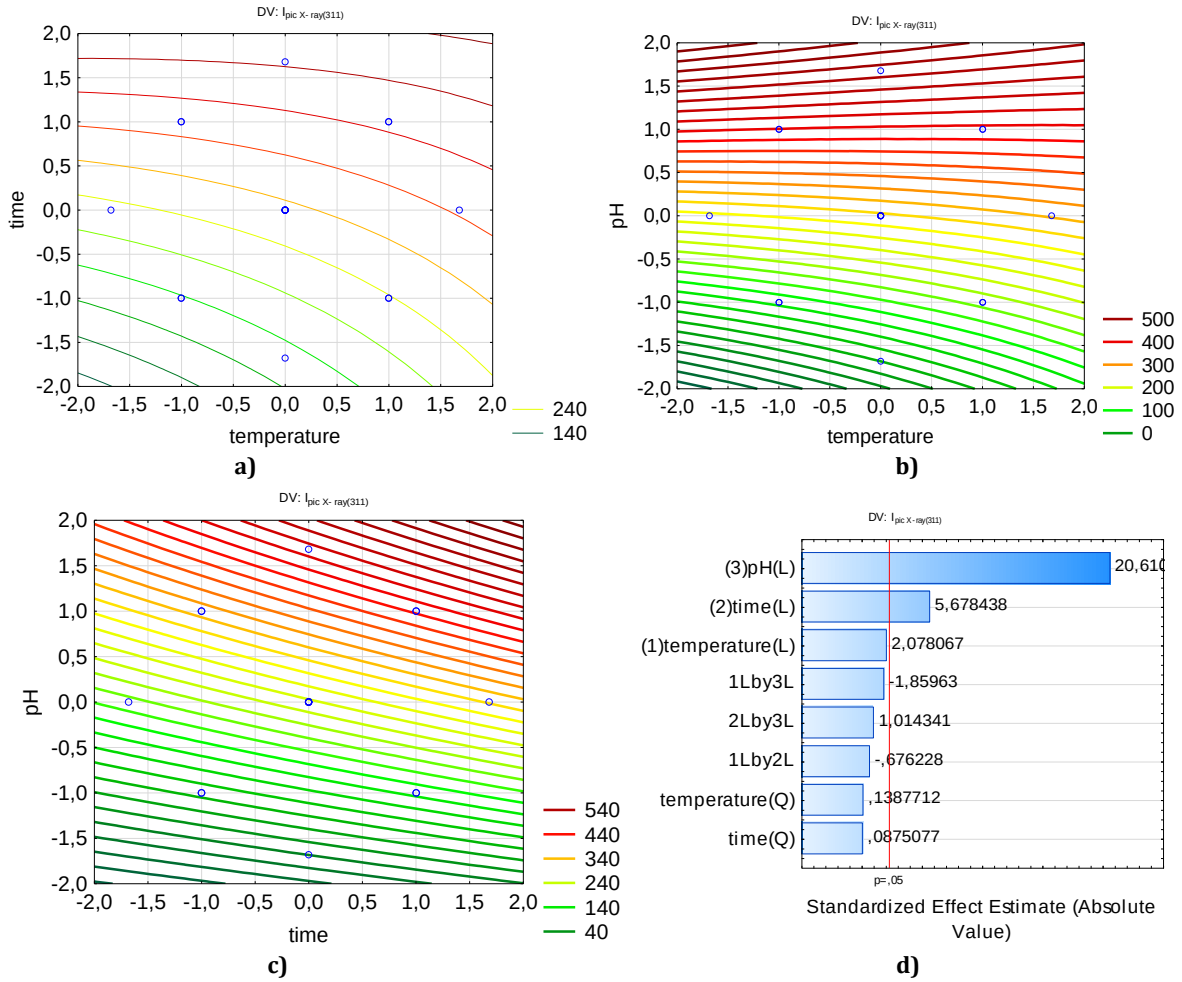

$$I_{X\text{-ray pic}} = 255.67 + 14.12\,x_1 + 38.58\,x_2 + 140.02x_3 - 6.01x_1x_2 - 16.5x_1x_3 + 9.02x_2x_3 \quad (4)$$

Fig. 2. Graphs of the dependence of the intensity of the peaks on the X-ray pattern along the line (311) on the synthesis parameters a- $I_{X\text{-ray pic}}=f(pH, \tau)$, b-$I_{X\text{-ray pic}}=f(pH, t)$, c- $I_{X\text{-ray pic}}= f(t, \tau)$ d -Paretto chart

The analysis of crystallite sizes (Table 3) shows that for powders obtained by the plasma-chemical method, they have values similar to those presented by other authors who used co-precipitation technologies for the production of cobalt ferrite [4; 6]. Fig. 3 shows the Pareto chart of standardized effects up to 95 % statistical significance (p = 0.05). Factors with absolute values higher than 2.1 are significant in terms of influence on the average size of powder crystallites.

Individual factors (pH, time) have a significant and positive effect on the average size of crystallites, temperature affects the size of crystallites much less. In the case of combined effects, only the interactions between pH and temperature and between pH and reaction time affect crystallite growth, with the interaction of pH and temperature having a negative effect.

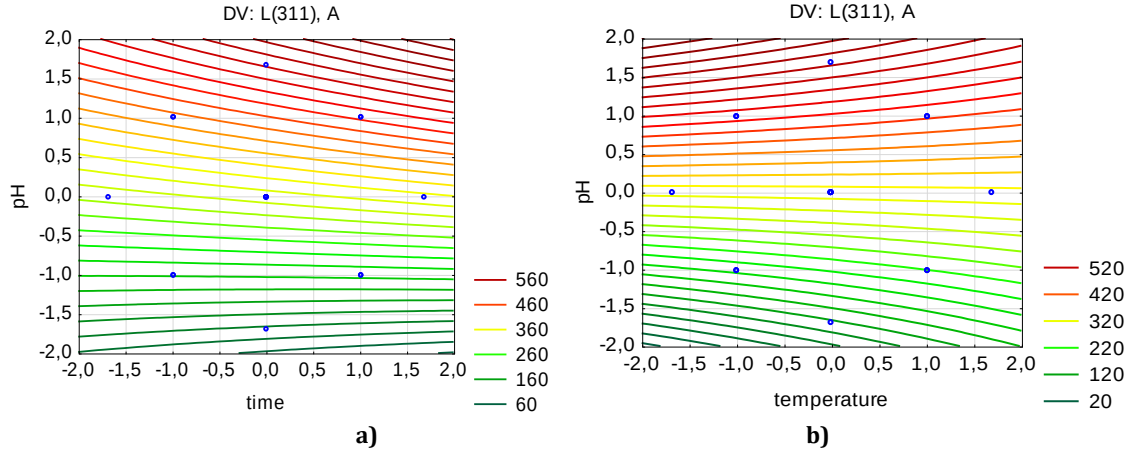

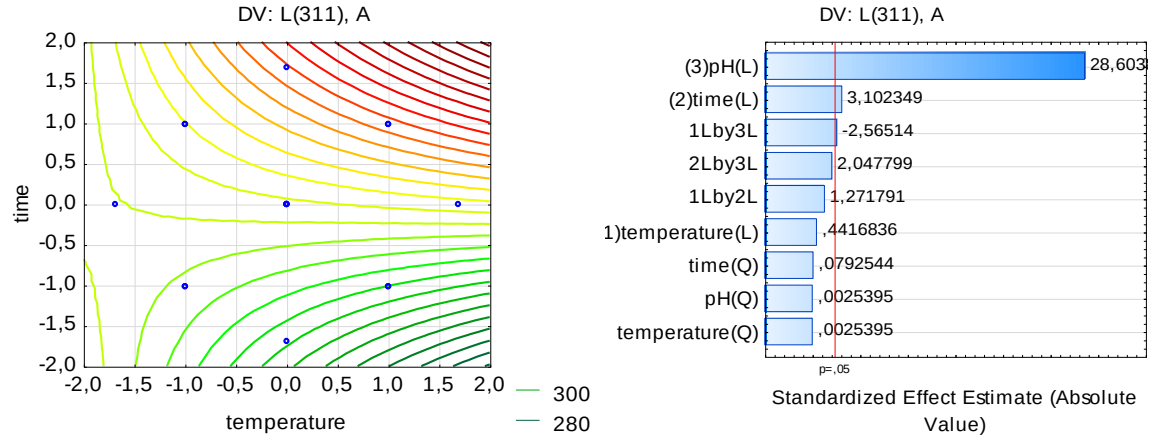

c) **d)**

$$L_{(311)} = 331.04 + 1.96\,x_1 + 13.78\,x_2 + 127.01x_3 - 7{,}37x_1x_2 - 14.87x_1x_3 + 11.88x_2x_3 \quad (5)$$

Fig. 3. Graphs of dependence of crystallite sizes along the (311) line on synthesis parameters a - L=f(pH, τ), b– L=f(pH, t),c- L=f(t, τ) d -Paretto chart

The mutual influence of variables on the size of crystallites is represented by isolines (Fig. 3). Fig. 3c shows that the contour lines have a significant curvature, which indicates a non-linear interaction between the variables (temperature and time). According to the shape of the contour lines, a decrease in the pH of the reaction medium from +2 to -2, as well as a decrease in the synthesis temperature from +2 to -2 leads to the formation of ferrite with a smaller crystallite size, a simultaneous increase in the level of these variables gives the opposite effect, regardless of the individual level of both parameters. Analyzing Fig. 3 a, b, it can be seen that there is an almost linear relationship between pH and temperature and pH and treatment time. In the interaction between pH and treatment time, the influence of pH prevails. Increasing the pH level from -2 to +2, as well as increasing the reaction time from -2 to +2 causes an increase in the crystallite size. In addition, for a fixed pH value of the reaction medium, the influence of the treatment time with a plasma discharge increases, which also contributes to the growth of crystallites. A mathematical model was developed on the basis of statistical analysis. The model is adequate, the correlation coefficient is $R^2 = 0.9892$.

The largest crystallite size (505–560 Å) can be obtained at high values of temperature and pH (temperature 40 ℃, time 20 minutes and pH 12). The smallest crystallite size (119–165 Å) was obtained at a temperature of 20 ℃and a minimum treatment time (5 minutes) and a pH of 10.

The regularities of changes in magnetic properties were studied by analyzing the constructed hysteresis curves. Magnetic characteristics are given in Table 3 and Fig. 4 (a, b, c, d).

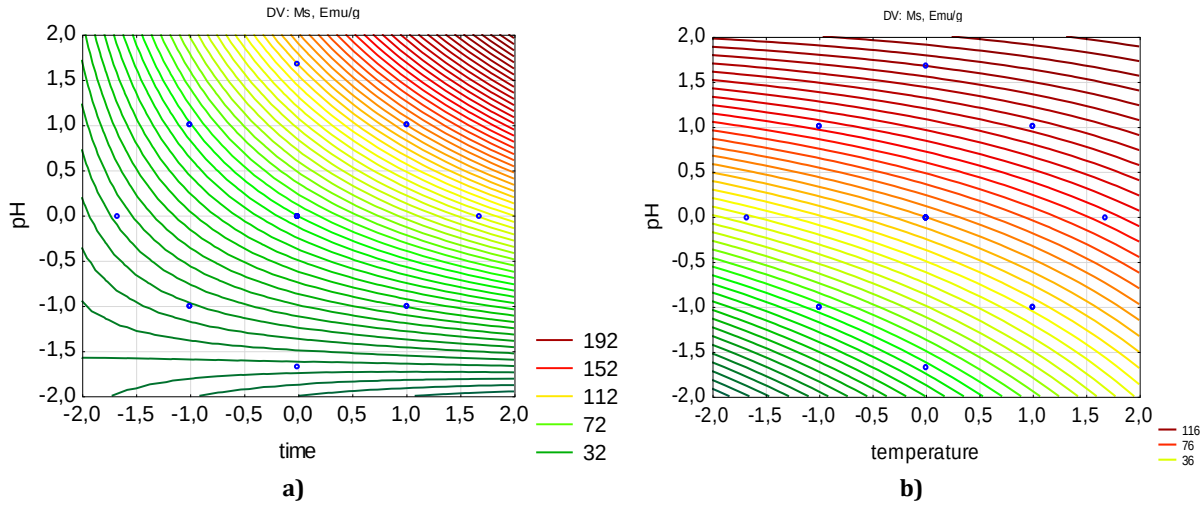

a) **b)**

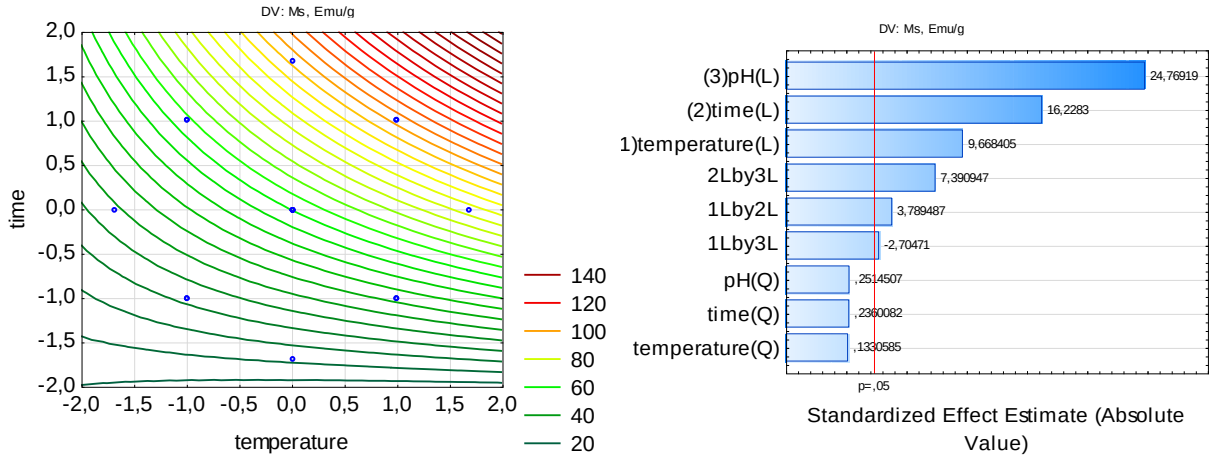

c) **d)**

$$Ms = 60.19 + 25.59\ x_1 + 42.95\ x_2 + 65.59x_3 + 13.1x_1x_2 - 9.35x_1x_3 + 25.55x_2x_3 \quad (6)$$

Fig. 4. Graphs of dependence of saturation magnetization on synthesis parameters a- Ms =f(pH, τ), b- Ms =f(pH, t),c- Ms =f(t, τ) d -Paretto chart

Fig. 4 shows that a high saturation magnetization (120–138 Emu/g) can be achieved at an elevated temperature of 40 °C and processing time (samples 1, 2). A high value of saturation magnetization is associated with the formation of cobalt ferrite with high crystallinity and large crystallite sizes. Lower saturation magnetization values (8.0–14 Emu/g) are due to the formation of non-magnetic impurity phases of iron oxides and oxyhydroxides (samples 6, 7, 8). Statistical processing showed that the standard deviation was 23.90 and the correlation coefficient R^2 was 0.99242, which confirmed the satisfactory description of the experimental data.

Dispersion analysis of the dependence of the dislocation density in the samples on the synthesis parameters showed that the samples obtained at a pH below 10 have a higher density of dislocations (Fig. 5a, b, c). Fig. 5 shows the Paretto diagram for the density of dislocations (cm^{-2}), which emphasizes that the pH of the reaction medium is an independent variable that has the greatest influence on the degree of defectiveness of the samples. Its increase contributes to the formation of a product with increased crystallinity and a defect-free structure. Temperature also affects the density of dislocations, a higher temperature reduces the defectiveness of the powder, increasing its quality. An increase in processing time and temperature has a positive effect on the quality of cobalt ferrite.

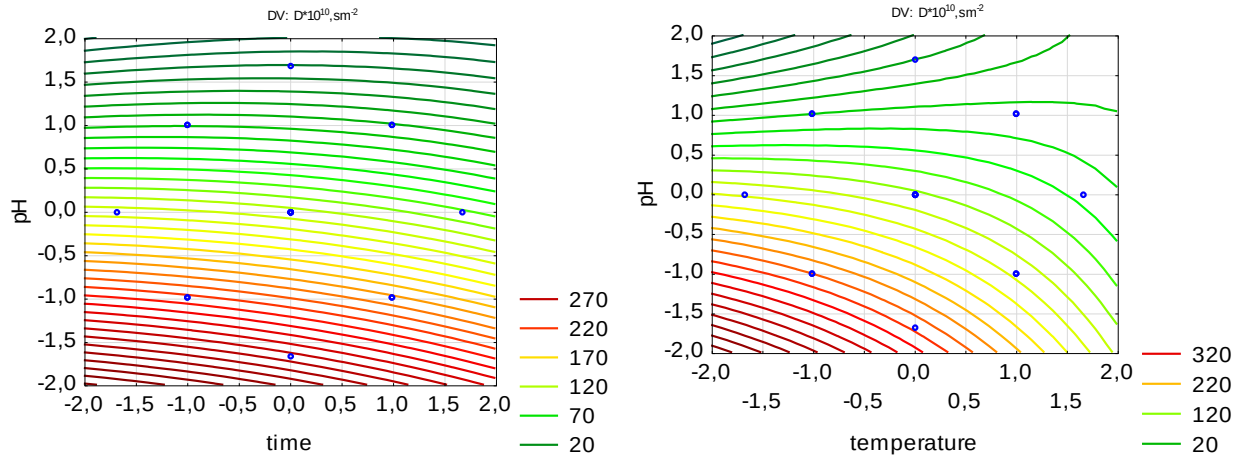

a) **b)**

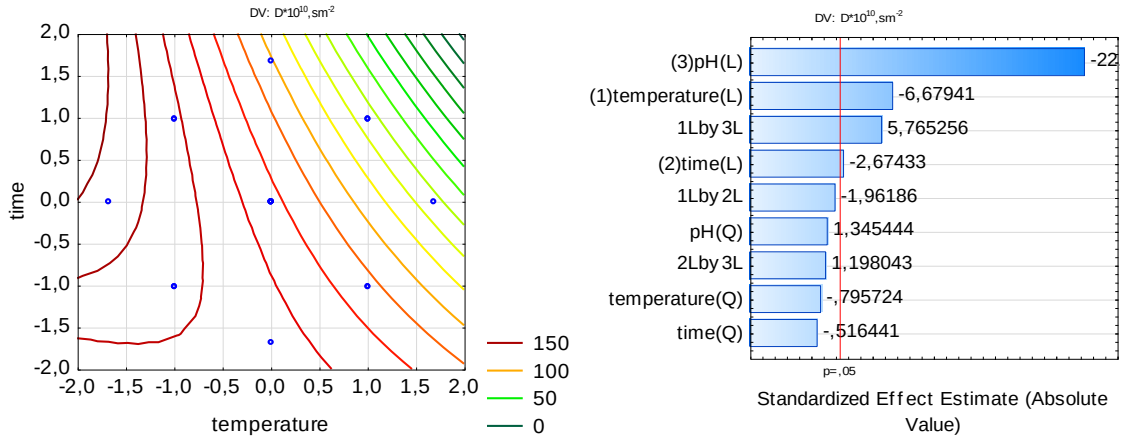

$$D = 123.12 - 24.44\,x_1 - 9.78\,x_2 - 81.77x_3 - 9.37x_1x_2 + 27.55x_1x_3 + 5.72x_2x_3 \quad (7)$$

Fig. 5. Graphs of dependence of dislocation density on synthesis parameters a- D=f(pH, τ), b-D=f(pH, t),c- D=f(t, τ) d -Paretto chart

The effect of pH on the density of dislocations is explained by the formation of a highly crystalline defect-free structure of cobalt ferrite. At solution pH less than 10, the oxidation process under the action of the plasma discharge occurs quickly with the formation of an amorphous defective structure. According to [32], the speed of the oxidation process is determined by the pH of the solution, other things being equal. Low pH values lead to the formation of non-magnetic phases (goethite, hematite). An increase in pH slows down the process of oxidation of Fe(II) hydroxo compounds to trivalent and leads to the formation of ferrite. This is confirmed by the dependence of magnetic characteristics on the pH of the initial suspension. This explains the symbiotic dependence between the values of saturation magnetization and the density of dislocations.

Conclusions

The influence of the synthesis parameters on the size of $CoFe_2O_4$ crystallites, the density of dislocations, saturation magnetization, intensity of peaks in X-ray diffraction patterns, and phase composition was determined using the central composite rotatable planning of the experiment.

It was established that the largest crystallite size (505–560 Å) was obtained at high temperature and pH values. The smallest crystallite size (119–165 Å) was obtained at a temperature of 20 ℃, a minimum treatment time of 5 minutes and a pH of 10.

Based on the analysis of hysteresis curves, it is shown that high saturation magnetization values (120–138 Emu/g) can be achieved at an elevated temperature of 40℃ and processing time. This is due to the formation of cobalt ferrite with high crystallinity and large crystallite sizes. Lower values of saturation magnetization (8.0–14 Emu/g) are due to the formation of non-magnetic impurity phases of iron oxides and oxyhydroxides.

The obtained experimental-statistical models describe well the obtained experimental data and were used for optimization of plasma chemical synthesis. That is, the study of the influence of synthesis parameters on the structure and magnetic properties makes it possible to effectively use plasma chemical synthesis to regulate the properties of $CoFe_2O_4$ nanoparticles for various applications.

References

[1] Liandi, A. R., Cahyana, A. H., Kusumah, A. J. F., Lupitasari, A., Alfariza, D. N., Nuraini, R., Sari, R. W., Kusumasari, F. C. (2023). Recent trends of spinel ferrites (MFe_2O_4: Mn, Co, Ni, Cu, Zn) applications as an environmentally friendly catalyst in multicomponent reactions: A review. *Case Studies in Chemical and Environmental Engineering*, 7, 100303. https://doi.org/10.1016/j.cscee.2023.100303

[2] Frolova, L. A., Khmelenko, O. V. (2021). The study of Co–Ni–Mn ferrites for the catalytic decomposition of 4-nitrophenol. *Catalysis Letters*, 151, 1522–1533. https://doi.org/10.1007/s10562-020-03419-1

[3] Rezaei, B., Yari, P., Sanders, S. M., Wang, H., Chugh, V. K., Liang, S., Shahriar Mostufa, S., Xu, K., Wang, J. P., Gómez-Pastora, J., Wu, K. (2023). Magnetic nanoparticles: a review on synthesis, characterization, functionalization, and biomedical applications. *Small*, *20*(5), 2304848. https://doi.org/10.1002/smll.202304848

[4] Bayça, F. (2024). Characterization and magnetic properties of $CoFe_2O_4$ nanoparticles synthesized by the co-precipitation method. *International Journal of*

Applied Ceramic Technology, 21(1), 544–554. https://doi.org/10.1111/ijac.14518

[5] Yu, L., Fan, Y., Li, C., Liu, C., Ren, X., Yang, H., Lin, S. (2023). Synthesis and characterization of highly efficient oil–water separation, recyclable, magnetic particles $CoFe_2O_4$/SDB. *Polymer Bulletin*, *80*(4), 3571–3584. doi:10.21203/rs.3.rs-601296/v1

[6] de Medeiros, F., Madigou, V., Lopes-Moriyama, A. L., de Souza, C. P., Leroux, C. (2020). Synthesis of $CoFe_2O_4$ nanocubes. *Nano-Structures & Nano-Objects,* 21, 100422. doi:10.1016/j.nanoso.2019.100422

[7] Frolova, L., Khmelenko, O. (2018). Investigation of the magnetic properties of ferrites in the CoO-NiO-ZnO using simplex-lattice design. *Journal of Nanomaterials*, 2018, 1–8. https://doi.org/10.1155/2018/5686741

[8] Malinowska, I., Ryżyńska, Z., Mrotek, E., Klimczuk, T., Zielińska-Jurek, A. (2020). Synthesis of $CoFe_2O_4$ nanoparticles: the effect of ionic strength, concentration, and precursor type on morphology and magnetic properties. *Journal of Nanomaterials*, *2020*, 1–12. https://doi.org/10.1155/2020/9046219

[9] Wei, K., Huai, H. X., Zhao, B., Zheng, J., Gao, G. Q., Zheng, X. Y., Wang, C. C. (2022). Facile synthesis of $CoFe_2O_4$ nanoparticles and their gas sensing properties. *Sensors and Actuators B: Chemical*, 369, 132279. http://dx.doi.org/10.1016/j.snb.2022.132279

[10] Alharthy, R. D., Saleh, A. (2021). A novel trace-level ammonia gas sensing based on flexible PAni-CoFe2O4 nanocomposite film at room temperature. *Polymers, 13*(18), 3077. https://doi.org/10.3390/polym13183077

[11] Chen, K., Li, Y., Du, Z., Hu, S., Huang, J., Shi, Z., Su, B., Yang, G. (2022). $CoFe_2O_4$ embedded bacterial cellulose for flexible, biodegradable, and self-powered electromagnetic sensor. *Nano Energy*, 102, 107740. DOI:10.2139/ssrn.4136294

[12] Ansari, M. A., Govindasamy, R., Begum, M. Y., Ghazwani, M., Alqahtani, A., Alomary, M. N., Jamous, Y. F., Alyahya, S. A., Asiri, S., Khan, F. A., Almessiere, M. A., Baykal, A. (2023). Bioinspired ferromagnetic $CoFe_2O_4$ nanoparticles: Potential pharmaceutical and medical applications. *Nanotechnology Reviews*, *12*(1), 20230575. doi:10.1515/ntrev-2023-0575

[13] Abimathi, N., Harshene, H., Vidhya, B. (2022). Synthesis and characterization of $CoFe_2O_4$ nanoparticles with its medical application. *Materials Today: Proceedings*, *62*(1-2), 2315–2319. doi:10.1016/j.matpr.2022.04.101

[14] Khizar, S., Ahmad, N. M., Ahmed, N., Manzoor, S., Hamayun, M. A., Naseer, N., Tenorio, M.K.L., Lebaz, N., Elaissari, A. (2020). Aminodextran coated $CoFe_2O_4$ nanoparticles for combined magnetic resonance imaging and hyperthermia. *Nanomaterials, 10*(11), 2182. https://doi.org/10.3390/nano10112182

[15] Frolova, L., Sukhyy, K. (2022). The effect of the cation in spinel ferrite $MeFe_2O_4$ (Me = Co, Ni, Mn) on the photocatalytic properties in the degradation of methylene blue. *Materials Today: Proceedings*, 62, 7726–7730. https://doi.org/10.1016/j.matpr.2022.03.503

[16] Frolova, L. (2020). Photocatalytic activity of spinel ferrites $Co_xFe_{3-x}O_4$ (0.25< x< 1) obtained by treatment contact low-temperature non-equilibrium plasma liquors. *Applied Nanoscience*, *10*(12), 4585. doi:10.1007/s13204-020-01344-8

[17] Sun, Q., Wu, S., Li, K., Han, B., Chen, Y., Pang, B., Yu, L., Dong, L. (2020). The favourable synergistic operation of photocatalysis and catalytic oxygen reduction reaction by a novel heterogeneous $CoFe_2O_4$-TiO_2 nanocomposite. *Applied Surface Science*, 516, 146142. DOI:10.1016/j.apsusc.2020.146142

[18] Faroughi Niya, H., Hazeri, N., Fatahpour, M. (2021). Synthesis, characterization, and application of $CoFe_2O_4$@amino-2-naphthol-4-sulfonic acid as a novel and reusable catalyst for the synthesis of spirochromene derivatives. *Applied Organometallic Chemistry*, *35*(3), e6119. https://doi.org/10.1002/aoc.6119

[19] Sharifianjazi, F., Moradi, M., Parvin, N., Nemati, A., Rad, A. J., Sheysi, N., Abouchenari, A., Mohammadi, A., Karbasi, S., Ahmadi, Z., Khanian, A. E., Irani, M., Pakseresht, A., Sahmani, S., Asl, M. S. (2020). Magnetic $CoFe_2O_4$ nanoparticles doped with metal ions: a review. *Ceramics International*, *46*(11), 18391–18412. doi:10.1016/j.ceramint.2020.04.202

[20] Ji, G., Tang, S., Xu, B., Gu, B., Du, Y. (2003). Synthesis of $CoFe_2O_4$ nanowire arrays by sol–gel template method. *Chemical physics letters*, *379*(5-6), 484–489. doi:10.1016/j.cplett.2003.08.090

[21] Kim, Y. I., Kim, D., Lee, C. S. (2003). Synthesis and characterization of $CoFe_2O_4$ magnetic nanoparticles prepared by temperature-controlled coprecipitation method. *Physica B: Condensed Matter*, *337*(1-4), 42–51. http://dx.doi.org/10.1016/S0921-4526(03)00322-3

[22] Gyergyek, S., Makovec, D., Kodre, A., Arčon, I., Jagodič, M., Drofenik, M. (2010). Influence of synthesis method on structural and magnetic properties of cobalt ferrite nanoparticles. *Journal of Nanoparticle Research*, 12, 1263–1273. doi:10.1007/s11051-009-9833-5

[23] Caldeira, L. E., Erhardt, C. S., Mariosi, F. R., Venturini, J., Zampiva, R. Y. S., Montedo, O. R. K., Arcaro, S., Bergmann C. P., Braganca, S. R. (2022). Correlation of synthesis parameters to the structural and magnetic properties of spinel cobalt ferrites ($CoFe_2O_4$)–an experimental and statistical study. *Journal of Magnetism and Magnetic Materials*, 550, 169128. doi:10.1016/j.jmmm.2022.169128

[24] Lavorato, G., Alzamora, M., Contreras, C., Burlandy, G., Litterst, F. J., Baggio-Saitovitch, E. (2019). Internal structure and magnetic properties in cobalt ferrite nanoparticles: Influence of the synthesis method. *Particle & Particle Systems Characterization*, *36*(4), 1900061. https://doi.org/10.1002/ppsc.201900061

[25] Senthil, V. P., Gajendiran, J., Raj, S. G., Shanmugavel, T., Kumar, G. R., Reddy, C. P. (2018). Study of structural and magnetic properties of cobalt ferrite ($CoFe_2O_4$) nanostructures. *Chemical Physics Letters*, 695, 19–23. http://dx.doi.org/10.1016/j.cplett.2018.01.057

[26] Bououdina, M., Manoharan, C. (2020). Dependence of structure/morphology on electrical/magnetic properties of hydrothermally synthesised cobalt ferrite nanoparticles. *Journal of Magnetism and Magnetic Materials*, 493, 165703. doi:10.1016/j.jmmm.2019.165703

[27] Purnama, B., Wijayanta, A. T., Suharyana, S. (2019). Effect of calcination temperature on structural and magnetic properties in cobalt ferrite nano particles. *Journal of King Saud University-Science*, *31*(4), 956–960. doi:10.1016/j.jksus.2018.07.019

[28] Frolova, L., Derimova, A., Khlopytskyi, A., Galivets, Y., & Savchenko, M. (2016). Investigation of phase formation in the system $Fe^{2+}/Co^{2+}/O_2/H_2O$. *Eastern-European*

Journal of Enterprise Technologies, 6(6), 64–68. https://doi.org/10.15587/1729-4061.2016.85123

[29] Frolova, L. A. (2014). Production conditions of iron oxide black from pickle liquors. *Metallurgical & Mining Industry*, (4), 65–69.

[30] Ravindra, A. V., Ju, S. (2023). Mesoporous $CoFe_2O_4$ nanocrystals: Rapid microwave-hydrothermal synthesis and effect of synthesis temperature on properties. *Materials Chemistry and Physics*, 303(1-7), 127818. doi:10.1016/j.matchemphys.2023.127818

[31] Frolova, L., Pivovarov, A., Tsepich, E. (2016). Non-equilibrium plasma-assisted hydrophaseferritization in Fe^{2+}–Ni^{2+}–SO_4^{2-}–OH^- System. *Nanophysics, Nanophotonics, Surface Studies, and Applications. Springer Proceedingsin Physics*, 183, 213–220. doi: 10.1007/978-3-319-30737-4_18

[32] Frolova, L., Sukhyy, K. (2022). Investigation of the ferritization process in the Co^{2+}–Fe^{2+}–SO_4^{2-}–OH^- system under the action of contact non-equilibrium low-temperature plasma. *Applied Nanoscience*, 1–8. https://doi.org/10.1007/s13204-021-01755-1